Evaporative cooling rubidium atoms with microwave radiation

Dezhi Xiong (熊德智), Pengjun Wang (王鹏军), Haixia Chen (陈海霞), and Jing Zhang (张 靖)*

State Key Laboratory of Quantum Optics and Quantum Optics Devices, Institute of Opto-Electronics, Shanxi University, Taiyuan 030006, China

**E-mail: jzhang74@yahoo.com*

Received August 11, 2009

We report the experimental achievement of ^{87}Rb Bose-Einstein condensation in a magnetic trap with microwave and radio frequency (RF) induced evaporation. Evaporative cooling is realized by using 6.8 GHz microwave radiation driving the ^{87}Rb atoms to transit from the ground-state hyperfine state $|F = 2, m_F = 2\rangle$ to $|F = 1, m_F = 1\rangle$. Compared with RF-induced evaporation, ^{87}Rb atoms are hardly to achieve pure condensate by microwave evaporation cooling due to the effect of atoms in the $|F = 1, m_F = 1\rangle$ state being pumped back into the trapping $|F = 2, m_F = 1\rangle$ state.

OCIS codes: 020.0020, 350.4010.

doi: 10.3788/COL20100804.0351.

Since the first experimental realization of the Bose-Einstein condensation (BEC)[1−3], ultracold atomic gases have achieved a lot of attention in experiment[4] and theory[5,6]. Especially, the observation of quantum degenerate Fermi gas (DFG) and quantum degenerate Bose-Fermi mixtures (BFM) provides new opportunities for understanding high-T_c superconductivity, strong interaction, and quantum many-body systems. Typically, evaporative cooling of atoms is still a crucial technique in reaching the quantum degenerate temperature for alkali atom gas. And sympathetic cooling is used to cool some species which cannot be efficiently cooled by direct evaporation, such as in the cases of ^{40}K[7] and ^{6}Li[8]. Usually, evaporative cooling can be fulfilled through several methods, such as lowering trap field, radio frequency (RF), and microwave (MW) techniques.

The advantage of radiative evaporation (RF and MW) is that we do not have to modify the magnetic potential, because the evaporative rate can be precisely controlled by the amplitude and frequency of the radiative field. For RF-induced evaporation, the RF radiation flip the atomic spin between $|F, m_F = i\rangle$ and $|F, m_F = i-1\rangle$ states. The resonance condition for magnetic field strength B is

$$g_F \mu_B B = \hbar\omega_{\rm RF}, \tag{1}$$

where g_F is landé factor, $\omega_{\rm RF}$ is the RF field frequency. For MW-induced evaporation, MW evaporation transfers atoms between Zeeman sublevels, which belong to different hyperfine levels of the ground states. The resonance condition for a transition between the hyperfine states $|F, m_F = i\rangle$ and $|F-1, m_F = i-1\rangle$ is

$$g_F\,(2m_F - 1)\,\mu_B B + \hbar\omega_{hf} = \hbar\omega_{\rm MW}, \tag{2}$$

where $\omega_{hf}/2\pi$ is the hyperfine splitting ($\sim$ 6.8 GHz for ^{87}Rb), and $\omega_{\rm MW}/2\pi$ is the MW frequency. MW radiation evaporation has been explored by many groups[4,8−13], which is utilized frequently in sympathetic cooling. Owing to the large difference in the hyperfine splittings of the different atoms, MW cooling method is species-selective and avoids any evaporative losses of the other species during the cooling process.

In this letter, we report on the production of ^{87}Rb BEC by evaporative cooling using MW-knife. The MW-knife is tuned to the hyperfine transition at 6.8 GHz, which induces transitions from trapped $|F = 2, m_F = 2\rangle$ state to untrapped $|F = 1, m_F = 1\rangle$ state. In the same initial condition, we also apply the RF radiation to the ^{87}Rb atoms. When the ^{87}Rb atoms are cooled down to critical temperature point, a lot of ^{87}Rb atoms are populated in the hyperfine state $|F = 2, m_F = 1\rangle$ due to atoms in the $|F = 1, m_F = 1\rangle$ state being pumped back into the trapping $|F = 2, m_F = 1\rangle$ state by the same MW radiation in the course of evaporation. Compared with RF-induced evaporation, it is difficult to achieve the pure Rb BEC with MW radiation evaporation.

Our experimental apparatus is based on double magneto-optical trap (MOT) apparatus, which has been described in detail previously[14−17]. In short, ^{87}Rb atoms are captured from a vapor background in the first MOT (MOT1) and then transferred into the second MOT (MOT2) which resides in glass cell with much lower background pressure, and loaded in a magnetic trap. The magnetic trap in our experiment consists of an Ioffe-Pritchard potential produced by three coils in quadrupole-Ioffe configuration (QUIC)[17,18]. The schematic of the coils for QUIC trap is shown in Fig. 1. The typical axial and radial oscillation frequency of Rb are $\nu_{\rm ax}$ = 16.3 Hz and $\nu_{\rm rad}$ = 179.3 Hz. In the QUIC, we can load $\sim 10^8$ Rb atoms with a temperature of about 300 μK. Evaporative cooling of ^{87}Rb is performed, and the evolution of sample is obtained by time of flight (TOF) absorption imaging.

The MW signal is produced by a MW signal generator (N5183 MXG, Agilent). Then the MW radiation is amplified up to 1 W by a power amplifier (ZVE-8G+ 2–8 GHz, Minicircuit) and delivered to ^{87}Rb atoms by a waveguide coaxial converter (HD-70WSMAK, Vector Telecom) and a waveguide (HD-70WAL150, Vector Telecom), as shown in Fig. 2. To avoid the feedback signal to damage the power amplifier, a coaxial isolator (H13-1FFF, Aerotek) is used between power amplifier and

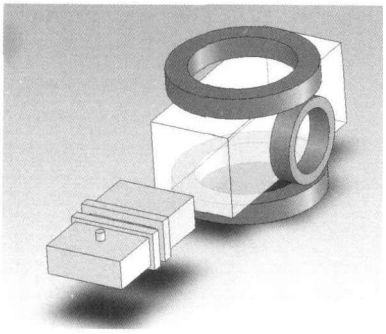

Fig. 1. Schematic of the experimental apparatus showing the magnetic trap setup, glass cell, and MW evaporation setup.

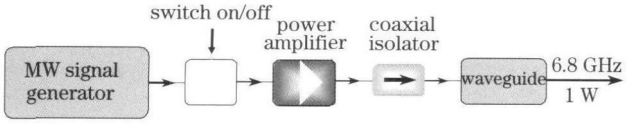

Fig. 2. Schematic of the MW radiation production and amplification.

coaxial converter. The frequency sweep and the MW switch are controlled and synchronized by a computer in the experiment. The distance between the mouth of the waveguide and ^{87}Rb atoms is about 15 cm.

After Rb atoms are prepared in their polarized spin state $|F = 2, m_F = 2\rangle$ and loaded in a QUIC trap, forced evaporative cooling of Rb is performed on the ground-state hyperfine transition between $|F = 2, m_F = 2\rangle$ and $|F = 1, m_F = 1\rangle$. The MW frequency is swept from 6.9 GHz to a final value of 6.8372 GHz in about 37.4 s. Figure 3 shows the absorption images of ^{87}Rb atoms at different MW knives. These images were taken with 1-ms expansion time and 60-μs exposure time. It is evident that the density of atomic gas increases when the evaporation terminates at different MW frequencies. By optimizing the MW power and sweeping frequency with real earnest, we find that the pure BEC is hard to be achieved at the end of the evaporation stage. At last we may achieve ^{87}Rb BEC including the condensate and thermal atoms with a total atomic number of 2.03×10^5, as shown in Fig. 4(b), where the number of condensate is 1.03×10^5. In the same initial condition, we could cool up to 3.0×10^5 ^{87}Rb atoms into a pure condensate by RF-induced evaporation, as shown in Fig. 4(a) with the final RF-knife frequency of 0.998 MHz. These results are caused by different evaporation mechanisms for the RF and MW-induced evaporation. For ^{87}Rb atoms, as shown in Fig. 5, RF radiation would induce a chain of transitions between different Zeeman sublevels starting from trapped states to untrapped state. Because of power broading and approximative linear width energy level among ^{87}Rb Zeeman sublevels, transitions between different Zeeman sublevels occur synchronously. This is a phenomenon of multi-photon transition. The RF field depletes all Zeeman sublevels of a target hyperfine state. The atoms are barely populated in the ground-state hyperfine state $|F = 2, m_F = 1\rangle$ in RF-induced evaporation cooling. However, MW evaporation is different. MW evaporation uses transition from the hyperfine state $|F = 2, m_F = 2\rangle$ to untrapped state $|F = 1, m_F = 1\rangle$. The important effect is that a small fraction of atoms in the high-seeker state $|F = 1, m_F = 1\rangle$ would transfer back to the $|F = 2, m_F = 1\rangle$ state[11,12] when they move towards a high magnetic field. It will affect the evaporation cooling due to many hot $|F = 2, m_F = 1\rangle$ atoms mixing with the $|F = 2, m_F = 2\rangle$ atoms. This problem may be solved by choosing the fixed MW carrier frequency, which is equal to the frequency between $|F = 2, m_F = 1\rangle$ and $|F = 1, m_F = 0\rangle$ state, such that it removes $|F = 2, m_F = 1\rangle$ atoms to $|F = 1, m_F = 0\rangle$ state. MW evaporation has a merit of Zeeman sublevel selective. It is very important in manipulating and purifying the magnetization of a mixture[10].

Figure 4 shows the BECs obtained by the use of RF and MW-induced evaporation. Figure 4(a) corresponds to the case of RF-induced evaporation where the image is

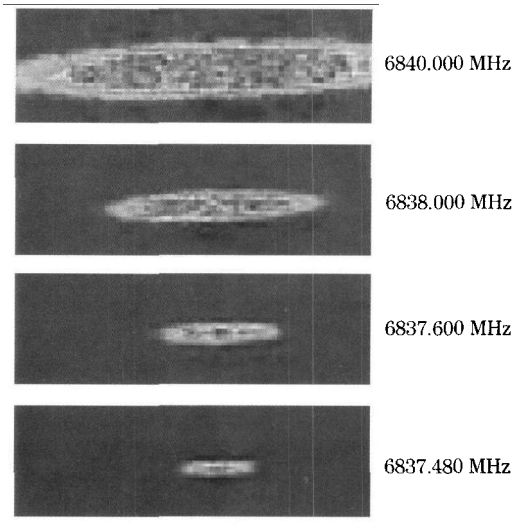

Fig. 3. Absorption images of ^{87}Rb atom groups at different end frequencies of the evaporation ramp.

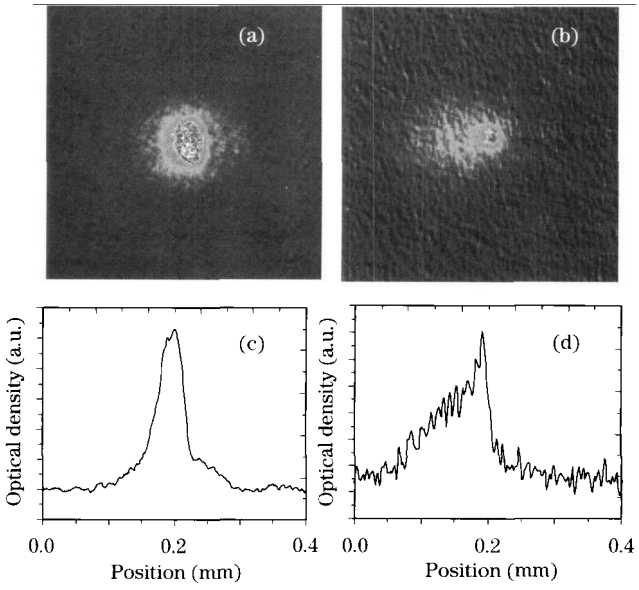

Fig. 4. Comparison between the BECs obtained by RF-induced evaporation and MW evaporation. (a) Two-dimensional (2D) image of the BEC obtained by RF-induced evaporation after 25-ms TOF; (b) (2D) image of the BEC obtained by MW evaporation after 30-ms TOF; (c) and (d) are vertically integrated column optical densities of images corresponding to (a) and (b) respectively.

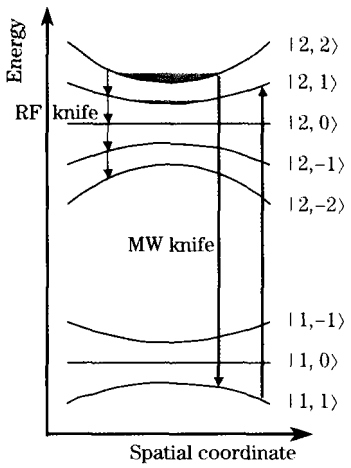

Fig. 5. Functional schematic of the RF and MW radiation evaporation. For ^{87}Rb atoms, RF evaporation induces transitions between different Zeeman sublevels belonging to the same hyperfine level of the ground states. And MW evaporation selectively uses transitions between Zeeman sublevels belonging to different hyperfine levels of the ground states.

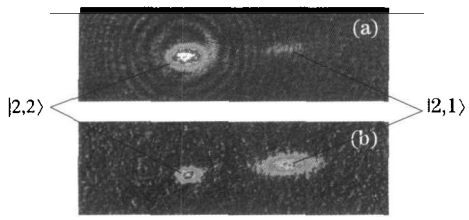

Fig. 6. Separation of the spin $|F = 2, m_F = 1\rangle$ state and $|F = 2, m_F = 2\rangle$ state when Rb BEC is achieved. (a) RF-induced evaporation; (b) MW evaporation.

taken with 25-ms expansion time and 60-μs exposure time, and Fig. 4(b) is MW evaporation where the image is taken with 30-ms expansion time and 60-μs exposure time. The vertically integrated column optical densities of Figs. 4(a) and (b) are respectively shown in Figs. 4(c) and (d). We also note that a lot of thermal cloud appears on the left of the condensate in Figs. 4(b) and (d) due to the slight difference of the switch-off time constant between the Ioffe and quadrupole coils during the process for the condensate being released from the QUIC trap. It is evident that most of the thermal atoms stay in the state $|F = 2, m_F = 1\rangle$. But these phenomena are unconspicuous in Figs. 4(a) and (c).

To ascertain the presence of the state $|F = 2, m_F = 1\rangle$ in Rb, by utilizing Stern-Gerlach effect, we let Rb atoms of different Zeeman substates separate in space, as shown in Fig. 6. The atoms in the state $|F = 2, m_F = 2\rangle$ lie in the left of the figure and the atoms in the state $|F = 2, m_F = 1\rangle$ in the right. Figure 6(a) shows the case of RF-induced evaporative cooling. It is obvious that the spin of atoms is almost in the $|F = 2, m_F = 2\rangle$ state, and only a little atoms stay in the $|F = 2, m_F = 1\rangle$ state. However, the result is very clear for MW radiative evaporative cooling, in which almost half of atoms stay in the $|F = 2, m_F = 1\rangle$ state, as shown in Fig. 6(b).

In conclusion, we have demonstrated MW radiation evaporation cooling of ^{87}Rb atoms and achieved BEC although the atoms with wrong Zeeman substate appear in the ultracold atoms. Comparing the RF-induced evaporation with the MW radiation evaporation, RF-induced evaporation cooling is adopted in our experiment realizing quantum degenerate Fermi mixture of ^{87}Rb and ^{40}K[17]. This will not affect the ^{40}K sample, while the presence of residual Rb atoms in the $|F = 2, m_F = 1\rangle$ Zeeman substate will give rise to inelastically collision losses if we adopt the MW radiation evaporation.

This work was supported in part by the National Natural Science Foundation of China for Distinguished Young Scholars (No. 10725416), National Basic Research Program of China (No. 2006CB921101), the National Natural Science Foundation of China for Excellent Research Team (No. 60821004), and the National Natural Science Foundation of China (No. 60678029).

References

1. M. H. Anderson, J. R. Ensher, M. R. Matthews, C. E. Wieman, and E. A. Cornell, Science **269,** 198 (1995).
2. K. B. Davis, M.-O. Mewes, M. R. Andrews, N. J. van Druten, D. S. Durfee, D. M. Kurn, and W. Ketterle, Phys. Rev. Lett. **75,** 3969 (1995).
3. C. C. Bardley, C. A. Sacket, J. J.Tollett, and R. G. Hulet, Phys. Rev. Lett. **75,** 1687 (1995).
4. Z. Hadzibabic, C. A. Stan, K. Dieckmann, S. Gupta, M. W. Zwierlein, A. Görlitz, and W. Ketterle, Phys. Rev. Lett. **88,** 160401 (2002).
5. A.-C. Ji, W. M. Liu, J. L. Song, and F. Zhou, Phys. Rev. Lett. **101,** 010402 (2008).
6. R. Qi, X.-L. Yu, Z. B. Li, and W. M. Liu, Phys. Rev. Lett. **102,** 185301 (2009).
7. B. DeMarco and D. S. Jin, Science **285,** 1703 (1999).
8. A. G. Truscott, K. E. Strecker, W. I. McAlexander, G. B. Partridge, and R. G. Hulet, Science **291,** 2570 (2001).
9. G. Modugno, G. Ferrari, G. Roati, R. J. Brecha, A. Simoni, and M. Inguscio, Science **294,** 1320 (2001).
10. D. Ciampini, E. Courtade, C. Sias, D. Cossart, G. Carelli, F. Mango, O. Morsch, and E. Arimondo, Opt. Commun. **257,** 340 (2006).
11. M. Hass, V. Leung, D. Frese, D. Haubrich, S. John, C. Weber, A. Rauschenbeutel, and A. Meschede, New J. Phys. **9,** 147 (2007).
12. C. Silber, S. Günther, C. Marzok, B. Deh, Ph. W. Courteille, and C. Zimmermann, Phys. Rev. Lett. **95,** 170408 (2005).
13. F. Schreck, L. Khaykovich, K. L. Corwin, G. Ferrari, T. Bourdel, J. Cubizolles, and C. Salomon, Phys. Rev. Lett. **87,** 080403 (2001).
14. D. Wei, D.-Z. Xiong, H.-X. Chen, and J. Zhang, Chin. Phys. Lett. **24,** 679 (2007).
15. D Wei, H.-X. Chen, D.-Z. Xiong, and J. Zhang, Acta Phys. Sin. (in Chinese) **55,** 6342 (2006).
16. D. Wei, D.-Z. Xiong, H.-X. Chen, P.-J. Wang, L. Guo. and J. Zhang, Chin. Phys. Lett. **24,** 1541 (2007).
17. D.-Z. Xiong, H.-X. Chen, P.-J. Wang, X.-D. Yu, F. Gao, and J. Zhang, Chin. Phys. Lett. **25,** 843 (2008).
18. P.-J. Wang, H.-X. Chen, D.-Z. Xiong, X.-D. Yu, F. Gao, and J. Zhang, Acta Phys. Sin. (in Chinese) **57,** 4840 (2008).